Interaction of Positive Pions with Hydrogen at 600 MeV*

PETER C. A. NEWCOMB
Lawrence Radiation Laboratory, University of California, Berkeley, California
(Received 7 June 1963)

The Berkeley 15-in. hydrogen bubble chamber was used to investigate π^+-p interactions at 600 MeV. There were 1738 good events, of which 71.9±0.8% were elastic. Partial waves up to at least $D_{5/2}$ are required to fit the elastic angular distribution. The inelastic events were almost entirely single-pion production. The ratio $(p+0)/(n++)$ was found to be 5.5±0.8 which agrees well with 4.9 predicted by the $(\frac{3}{2}, \frac{3}{2})$ pion-nucleon isobar model of Olsson and Yodh. It is also consistent with 6.5 predicted by Sternheimer and Lindenbaum. The pion momentum spectra and the $\pi-\pi$ Q-value distributions also support the Olsson and Yodh model. Thus the $(\frac{3}{2}, \frac{3}{2})$ pion-nucleon isobar is apparently the principal mechanism for single-pion production at 600 MeV. Angular distributions for the single-pion-production data are presented.

I. INTRODUCTION

AT 600 MeV there is a peak in the π^--p total cross section but not in that of the π^+-p system.[1,2] Therefore, if this peak is a resonance, it must have an isotopic spin, T, of $\frac{1}{2}$. To determine the $T=\frac{1}{2}$ phase shifts from the π^--p data, one must first ascertain the $T=\frac{3}{2}$ phase shifts from the π^+-p data at the same energy.[3] For this reason, 600 MeV was chosen as the beam energy for the present experiment.

In this experiment both the elastic and inelastic π^+-p interactions were investigated. From the 1245 elastic events obtained, the elastic angular distribution was quite accurately determined; however, there were not enough double scatters to study the polarization of the outgoing proton.

For inelastic interactions the energy of the incident beam is below the threshold for strange-particle production; only pion production is possible. Although kinematics permits as high as triple-pion production, the inelastic cross section is, in fact, almost entirely single-pion production. The question arises as to which of the known resonances might contribute to the two possible single-pion-production reactions:

$$\pi^++p\rightarrow\pi^++p+\pi^0,$$
$$\pi^++p\rightarrow\pi^++n+\pi^+.$$

There are two obvious possibilities: either a two-pion resonance, or the $(\frac{3}{2}, \frac{3}{2})$ pion-nucleon isobar. In this experiment the possible total mass of the two pions (<574 MeV) and their isotopic spin states preclude all of the established two-pion resonances.[4] This leaves the $(\frac{3}{2}, \frac{3}{2})$ pion-nucleon isobar, which has a mass of 1238 MeV, a Γ value of approximately 145 MeV, and can contribute to both reactions. In the present experiment the pion-nucleon total mass can lie between 1073 and 1377 MeV. Thus, the isobar dominates the available phase space and probably plays an important role in single-pion production.

Bergia *et al.*[5] have reformulated the isobar model of Sternheimer and Lindenbaum.[6] Two amplitudes can be formed with the isobar for the reaction $\pi^++p\rightarrow\pi^++p+\pi^0$. See Fig. 1. Bergia *et al.* point out that these two diagrams are indistinguishable experimentally, and therefore their amplitudes, not their cross sections, should be added:

$$d\sigma\approx|\alpha M_a+\beta M_b|^2\rho,$$

where α and β are the isotopic-spin Clebsch-Gordan coefficients, and ρ is a symbol for the phase-space factors. Bergia *et al.* used a theoretical expression to describe the effect of the isobar in M_a and M_b derived from the one that had successfully described the (3, 3) elastic resonance. To simplify the calculation of the momentum spectra of the two outgoing pions, they assumed that the N^* production was isotropic and that it decayed isotropically in its own rest frame. In their results the interference term produced a large dip in the momentum spectra of the outgoing pions. They state that if the interference term is neglected, their model reduces to the Sternheimer and Lindenbaum model, which corresponds to combining cross sections instead of amplitudes.

Recently Olsson and Yodh[7] have elaborated on the calculations of Bergia *et al.* by (a) using the proper decay angular distribution of the isobar and (b) by Bose symmetrizing the amplitude. The isobar production is still assumed to be in the S state. These authors find that by imposing these additional requirements, the large dips in the pion-momentum spectra found by Bergia *et al.* dissappear.

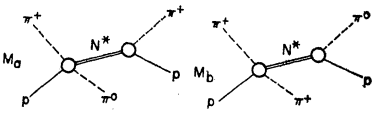

FIG. 1. The two amplitudes for the reaction $\pi^++p\rightarrow\pi^++p+\pi^0$ formed with the $(\frac{3}{2}, \frac{3}{2})$ isobar.

* This work was done under the auspices of the U. S. Atomic Energy Commission.

[1] J. Brisson, J. Detoeuf, P. Falk-Vairant, L. van Rossum, G. Valladas, and L. Yuan, Phys. Rev. Letters **3**, 561 (1959).

[2] T. Devlin, B. Moyer, and V. Perez-Mendez, Phys. Rev. **125**, 690 (1962).

[3] J. Ashkin, Suppl. Nuovo Cimento **14**, 221 (1959).

[4] The literature was searched up to January 1963.

[5] S. Bergia, F. Bonsignori, and A. Stanghellini, Nuovo Cimento **16**, 1073 (1960).

[6] R. M. Sternheimer and S. J. Lindenbaum, Phys. Rev. **109**, 1723 (1958). These authors give a complete list of references on this model in *ibid.* **123**, 333 (1961).

[7] M. Olsson and G. B. Yodh, Phys. Rev. Letters **10**, 353 (1963).

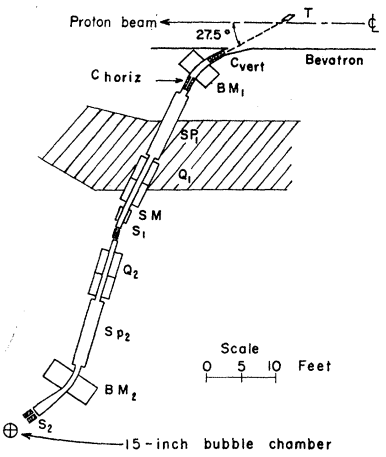

FIG. 2. Layout of the separated π^+ beam. The π^+ beam from the target (T) was focused by the quadrupole Q_1 onto slit S_1. The momentum was selected by bending magnet BM_1, and the subsequent mass separation by the crossed electric and magnetic fields in spectrometer SP_1. The second stage was essentially a mirror image of the first. The steering magnet SM was introduced for additional freedom in the horizontal plane. Horizontal and vertical collimators are C_{horiz} and C_{vert}, respectively.

II. EXPERIMENTAL PROCEDURE

This experiment was done at the Bevatron in the Berkeley 15-in. hydrogen bubble chamber. The beam which was built originally as a separated K^+ beam (see Goldhaber *et al.*[8]), was retuned to separate π^+ mesons. No change in the construction or layout of the apparatus was required. The layout is shown in Fig. 2. The circulating proton beam in the Bevatron was reduced to 10^9 protons per pulse in order to obtain a flux of about 25 π^+ mesons per pulse in the bubble chamber. Approximately 17 900 pictures were taken. Goldhaber *et al.* have described the beam and its operation in detail, so it will not be described here.

The beam momentum was checked by stopping protons in copper directly in front of the chamber. This gave 725±7-MeV/c pions at the center of the chamber. The quoted error is the uncertainty in the central value. In the data analysis a beam momentum of 725±13 MeV/c (kinetic energy of 599±13 MeV) at the center of the chamber was used. The ±13 MeV/c was the actual momentum spread given by Goldhaber *et al.* The central value was also verified by curvature measurements of the incoming beam tracks in the bubble chamber (see Fig. 3). The errors in the curvature measurements were too large to check the momentum spread of the beam.

The only non-negligible contamination in the beam was the μ^+ contamination, an estimated 10%. Since no absolute cross sections were measured in this experiment, the μ^+ contamination has no effect on the results.

III. TREATMENT OF DATA

A. Scanning

Two scintillation counters, operated in coincidence directly upbeam from the bubble chamber, counted the number of particles entering the chamber. This information was displayed on a pair of meters which were photographed with the bubble chamber. Scanners rejected pictures in which these counters showed greater than 35 counts. They also rejected poor quality pictures or those for which the counters were accidently turned off. In the whole experiment, 22.6% of the pictures, including pictures which had no tracks at all, were rejected; however, by far the greatest cause for rejection was too great a beam flux.

A rectangular fiducial region approximately 20 cm by 20 cm was defined in one view. Defining the fiducial region in only one view was convenient for scanning and was supplemented by much more restrictive criteria after the events were measured. The clearance between the fiducial region and the edge of the bubble chamber was approximately 8 cm at the ends and 5 cm on the sides.

The pictures were scanned for all interactions of beam tracks inside the fiducial region. All events except single-prong forward scatters were measured on a digitized microscope. There were 2494±1 of these, of which all but 8 had two outgoing prongs.

The film was scanned by two people, who also double-

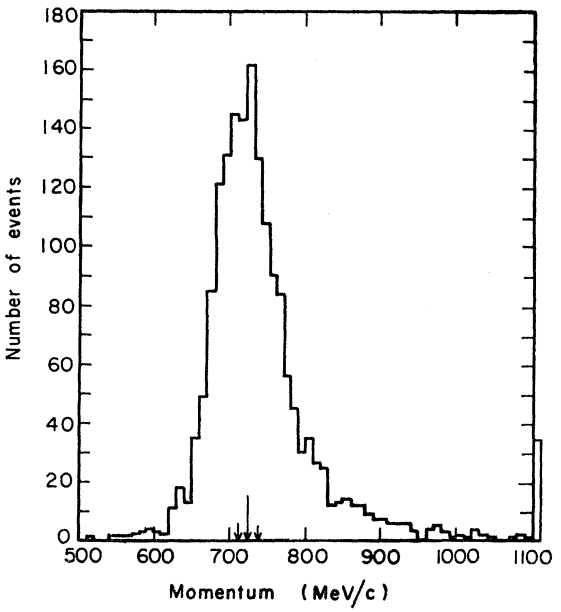

FIG. 3. Histogram of the measured momentum of the incoming pion of the 1245 elastic events and the 493 single-pion-production events. The arrows indicate 725±13 MeV/c.

[8] G. Goldhaber, S. Goldhaber, J. Kakyk, T. Stubbs, D. Stork, and H. Ticho, Lawrence Radiation Laboratory Document UCID-1250, 1960 (unpublished). For a brief summary see T. Stubbs, H. Bradner, W. Chinowsky, G. Goldhaber, S. Goldhaber, W. Slater, D. Stork, and H. Ticho, Phys. Rev. Letters 7, 188 (1961).

scanned 22% of the pictures to determine their scanning efficiencies. To find any possible errors, the writer, who was one of the scanners, looked at least twice at all of the events that were found.

The average scanning efficiency for the experiment was greater than 95%. No scanning bias was found for inelastic events. A scanning bias was observed, however, for elastic events in the forward direction. This bias was not large, and was well determined. The details will be explained in the Sec. IIID.

B. Computer Analysis of Data

The data were analyzed by using the FOG-CLOUDY-FAIR programs on an IBM-7090 computer.[9] Figure 4 shows the coordinate system used.

The fitting procedure and error assignments used in the CLOUDY program were checked by plotting the S-variable[10] distributions for 152 elastic events that fitted elasticity with $\chi^2 \leqslant 13.0$. The results were very good; therefore, the error assignments used in CLOUDY were not adjusted in any way. That is, the assigned measurement errors were arrived at on a definite physical basis.

1. Beam Editing and Beam Criteria

CLOUDY substituted a value of 730 MeV/$c\pm1.8\%$ for the momentum of every beam track at a point 19-cm upbeam from the center of the chamber ($x=-19.0$ cm). It then corrected for the ionization loss down to the point of interaction. This procedure gave 725 MeV/c $\pm1.8\%$ at the geometrical center of the chamber.

Histograms were made of α, β, y, and z for the incoming tracks which led to the following beam criteria for $x=-19.0$ cm:

$$\begin{aligned} &87.5 \text{ deg} \leqslant \alpha < 93.0 \text{ deg}, \\ &3.0 \text{ deg} \leqslant \beta < 10.0 \text{ deg}, \\ &-2.0 \text{ cm} \leqslant z < 3.0 \text{ cm}. \end{aligned} \tag{1}$$

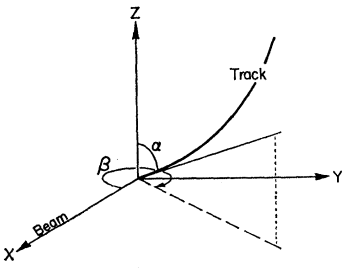

FIG. 4. The coordinate system used in FOG-CLOUDY-FAIR. The z-axis points towards the cameras.

[9] FOG and CLOUDY-FAIR Data-Processing-System Reference Manuals, Lawrence Radiation Laboratory Document UCID-1340, 1961 (unpublished).

[10] The S variables are defined such that if the measurement errors are correctly assigned and their distributions are Gaussian, and if there is no bias in the measurements, then the distribution of each S variable is Gaussian with a mean of zero and a standard deviation of unity. See J. P. Berge, F. T. Solmitz, and H. D. Taft, Rev. Sci. Instr. **32**, 538 (1961).

The median plane of the chamber in the z direction was $z=0$. There was a condition on y also; however, it merely redefined the scanning-table criterion and did not eliminate any events.

Since the elastic and inelastic π^+-p cross sections are quite strongly energy-dependent in the region of this experiment, a criterion was imposed directly on the measured value of the momentum of the incoming track. The criterion was

$$P_{\text{cen}}(1+DP_{\text{ext}}) \gtrsim 700 \text{ MeV}/c, \tag{2}$$

where P_{cen} is the measured momentum at the center of the incoming track. DP_{ext} is the relative external error. It consists of both the error due to multiple scattering and an expected average error made in measuring the position of the points along the track. CLOUDY also computed DP_{int}, the internal error, which was the relative error in the momentum based on the departure of the actual measured points from the arc of a circle. DP_{int} was used to judge the quality of the measurements (see Sec. IIIC).

2. Kinematic Analysis

The two-prong events were divided into two categories, E and N. Events in category N were obviously inelastic from their appearance on the scan table. That is, both outgoing prongs were on the same side of the incoming track, or comparison of two views showed conclusively that the event had to be noncoplanar. Events in category E then were either elastic or inelastic. CLOUDY fitted the two categories of events as follows:

Category E

$$\begin{aligned} \pi^+ + p &\rightarrow \pi^+ + p \\ &\rightarrow \pi^+ + p + \pi^0 \\ &\rightarrow \pi^+ + n + \pi^+ \end{aligned} \tag{3}$$

Category N

$$\begin{aligned} \pi^+ + p &\rightarrow \pi^+ + p + \pi^0 \\ &\rightarrow \pi^+ + n + \pi^+. \end{aligned}$$

In fitting each of these reactions CLOUDY tried all possible mass permutations of the outgoing particles. Only six events were found with more than two outgoing prongs, so multiple pion production was neglected.

C. Acceptance and Classification

Events were accepted and classified one at a time. Beam criteria (1) and (2), were applied to the FOG-CLOUDY-FAIR output, and the measured quantities for each event were checked roughly on the scan table. Any questionable measurements were repeated. The relative ionization as seen on the scan table was used to separate protons from pions. This was a very simple procedure since almost all outgoing tracks had momenta such that if they were pions they were minimum, and if they were protons they were well above minimum. In the very few cases where there was any doubt about the

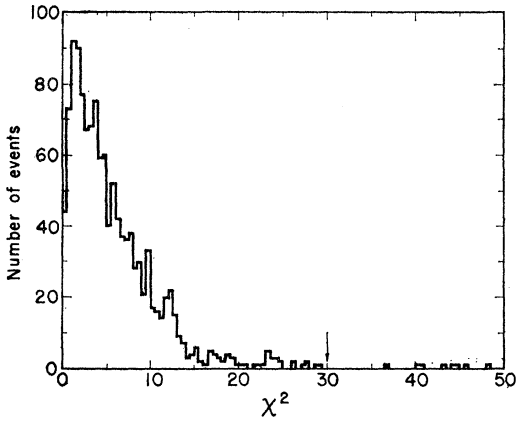

FIG. 5. Histogram of χ^2 for the elastic events. The cutoff was set at $\chi^2=30.0$. There are 1245 events with $\chi^2 \leqslant 30.0$.

mass of a particle, both possibilities were considered. It was assumed, of course, that all interactions were on hydrogen, so there could not be more than one outgoing proton. Tracks that stopped in the chamber were protons. Tracks that went backward in the laboratory system were counted as pions because kinematics prevents the proton from going backward.

Up to this point the data for the events were checked by a professional scanner. The writer then checked on the scanning table all events that failed to fulfill the beam criteria, or for which a possible error had been found, and made the final decision on each of them.

After the mass had been assigned to each of the two outgoing prongs, the writer checked the output further. If DP_{int} was greater than DP_{ext} for a given track, the track was checked again on the scan table for errors in its angles or curvature. If DP_{int} and DP_{ext} were both greater than 10%, and DP_{int} greater than twice DP_{ext}, the event was remeasured, unless a definite reason for the relatively large DP_{int} could be found at the scan table, such as turbulence or a very steep track.

Events that survived the above scrutiny were separated into elastic or single-pion production categories on the basis of their χ^2 values. An event was required not only to fit the category into which it was finally put, but also to not fit any other category permitted by the mass assignment. The final results of the separation were

$$\begin{aligned} &\pi^+ + p \rightarrow \pi^+ + p, && 1245 \text{ events} \\ &\pi^+ + p \rightarrow \pi^+ + p + \pi^0, && 418 \text{ events} \\ &\pi^+ + p \rightarrow \pi^+ + n + \pi^+, && 75 \text{ events} \end{aligned}$$

and the remaining events did not cause any bias as will be shown.

For the 1245 elastic events, χ^2 (elastic) was $\leqslant 30.0$; when these events were fitted as single-pion-production (1π) events, χ^2 was nonconvergent[11] except for nine events where the program converged for a different but possible mass assignment. Of these nine events, five had $\chi^2(1\pi)>37.0$; for the remaining four $\chi^2(1\pi)$ was 20.2, 15.5, 14.9, and 11.5. These last four events were separated by comparing elastic and inelastic χ^2 values and demanding that the constrained momenta agree with the curvature and ionization observed on the scan table. The χ^2 distribution for the elastic events is shown in Fig. 5. It has the general shape of the theoretical χ^2 distribution for four degrees of freedom,[12] but the tail is considerably broader than it should be.

The 418 events of the type $\pi^+ + p \rightarrow \pi^+ + p + \pi^0$ satisfied $\chi^2(1\pi) \leqslant 15.0$ and $\chi^2(\text{elastic}) \geqslant 100$. For most of these events χ^2(elastic) was >1000. There was only one event permitted by the ionization to fit both $\pi^+ p \pi^0$ and $\pi^+ n \pi^+$, and for which the program converged for both possibilities. The values of χ^2 were 0.2 and 21.6, respectively, which made the choice obvious.

Seventy-five events of the type $\pi^+ + p \rightarrow \pi^+ + \pi^+ + n$ also satisfied $\chi^2(1\pi) \leqslant 15.0$. There were no events in this category for which the program converged for another possible mass assignment. The χ^2 distribution for the inelastic events (Fig. 6) has the same general shape as the theoretical χ^2 distribution for one degree of freedom, but again the tail is too broad.[12]

Of the 2494 events that were observed at the scan table, 474 failed one or more of the beam criteria and were rejected. As already stated, 1738 events were either elastic or single-pion production events. The remaining 282 events were not used and fell into several categories. Each category was tested for any indication of a bias as compared to the 1738 events that were used. The purpose of checking for biases was to make certain that these 282 events were sufficiently random so that leaving them out did not bias the final results.

There were 49 events that did not fit any of the three

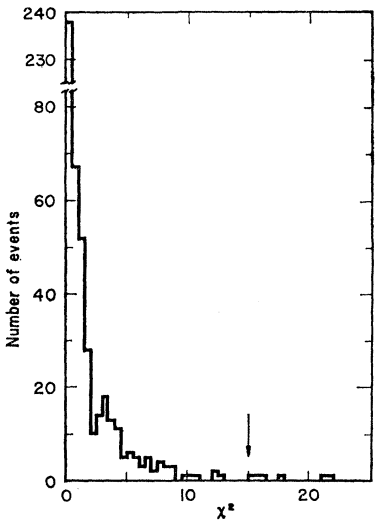

FIG. 6. Histogram of χ^2 for the inelastic events. The cutoff was set at $\chi^2=15.0$. There are 493 events with $\chi^2 \leqslant 15.0$.

[11] "Nonconvergent" means that the program was unable to minimize χ^2 in a manner consistent with energy and momentum conservation.

[12] H. Cramer, *Mathematical Methods of Statistics* (Princeton University Press, Princeton, 1958), pp. 233–236.

possible categories. Several checks were made to determine if these events showed any systematic difference from the events that were used. (a) There was no bias in the ratio of the number of events with an outgoing proton to those without. (b) The angular distribution of the outgoing π^+ for those of the 49 events which were in scanning category E (see Sec. IIIB 2) and which had an outgoing proton, had the same general features as the elastic angular distribution. This is what one would expect. (c) The ratio of the number of events in scanning category E to those in N was the same as for the experiment as a whole. From these three checks it was concluded that the 49 events were unbiased, and that neglecting them would not cause a bias in the experiment. This group of events probably resulted primarily from measurement difficulties, arising either in the chamber (small-angle scatters, turbulence, etc.) or in the digitized microscope.

Seventeen events fitted more than one category. For example, an event with $\chi^2(1\pi)\leqslant 15$ and $\chi^2(\text{elastic})\leqslant 100$ would fall into this group. No significant biases were found when this group was checked in the same way as the previous group of 49 events. The number of events in this group compared to the total number (1738) of events used represents the uncertainty in separating the three reactions. However, since this group of events shows no significant bias, there are too few of them to affect the errors in the branching ratios.

The remaining events, which fell into several lesser categories, were checked for biases in a manner similar to that already described, and no significant biases could be found.

D. Corrections

No biases were detected as a result of the separation of the events. However, it was still necessary to correct for scanning efficiency and for any bias in the azimuthal angle, Φ. Angle Φ lies between the z axis and the projection of the given outgoing track onto the plane perpendicular to the beam track, where the beam track is in a plane parallel to the x–y plane.

Elastic events were treated separately from inelastic events.

1. Elastic Events

The angular distribution was plotted as a function of the cosine of the pion scattering angle in the c.m. frame ($\cos\theta_{\text{c.m.}}$). A cut in the forward direction was made that required $\cos\theta_{\text{c.m.}}\leqslant 0.95$. At the upper limit this corresponds to a pion scattering angle of 11.3 deg in the laboratory system and a proton range of 0.95 cm. When projected onto the film, this angle and range correspond to: 11.3 to 1.5 deg, and 0.95 to 0.13 cm, respectively, depending on the angle Φ of the outgoing pion. Now, 1.5 deg and 0.13 cm correspond very closely to the smallest angle and track length that can be readily detected. Consequently, for $\cos\theta_{\text{c.m.}}\leqslant 0.95$ any Φ bias should not be large.

The angular distribution was divided into several intervals in $\cos\theta_{\text{c.m.}}$ and the Φ distribution folded into one quadrant was plotted for each interval. For $\cos\theta_{\text{c.m.}}<0.85$, none of these folded-$\Phi$ distributions showed any bias. For the interval $0.85\leqslant\cos\theta_{\text{c.m.}}<0.90$ there was a small indication of a Φ bias. The interval $0.90\leqslant\cos\theta_{\text{c.m.}}\leqslant 0.95$ showed a definite, although not very large, Φ bias. The correction appeared to be about 21 events for the 96 events that had been observed.

Two hundred and sixty one elastic events with $\cos\theta_{\text{c.m.}}\leqslant 0.95$ were found in the film that was double-scanned. For the sake of discussion we will refer to the two scanners as A and B. Of the 261 events, A found one event that B had missed, while B found 12 events that A had missed. The latter 12 events were studied as a function of $\cos\theta_{\text{c.m.}}$ and folded Φ. As a result, for $0.85\leqslant\cos\theta_{\text{c.m.}}\leqslant 0.95$ the scanning bias corresponded to a Φ bias, while for $\cos\theta_{\text{c.m.}}<0.85$ the scanning efficiency did not depend on folded Φ. Therefore, for $\cos\theta_{\text{c.m.}}<0.85$ the usual random scanning efficiency and correction to the data was calculated for each column in the histogram of $\cos\theta_{\text{c.m.}}$. Only three columns had efficiencies of less than 100% and required corrections, and even these were small (see Table I). For $0.85\leqslant\cos\theta_{\text{c.m.}}\leqslant 0.95$ each of the two columns was corrected for a folded-Φ bias. These corrections, which were six and 21 events [see Fig. 7(a) and (b)] were actually made on the basis of the folded-Φ distributions broken down according to scanner, as well as for the data collectively.

TABLE I. Experimental data for the elastic angular distribution.

Interval in $\cos\theta_{\text{c.m.}}$	Number of events observed	Correction	Final number of events	Uncertainty (events)
−1.0 to −0.9	5		5	2.77
−0.9 to −0.8	8		8	3.35
−0.8 to −0.7	11		11	3.84
−0.7 to −0.6	9		9	3.52
−0.6 to −0.5	9		9	3.52
−0.5 to −0.4	0		0	0.92
−0.4 to −0.3	4		4	2.53
−0.3 to −0.2	8		8	3.35
−0.2 to −0.1	10		10	3.68
−0.1 to 0	14		14	4.26
0 to 0.1	27		27	5.20
0.1 to 0.2	41		41	6.40
0.2 to 0.3	62		62	7.87
0.3 to 0.4	66		66	8.12
0.4 to 0.5	128	3	131	13.04
0.5 to 0.6	144		144	12.00
0.6 to 0.7	157	1	158	13.53
0.7 to 0.8	179	8	187	16.21
0.8 to 0.9	201	6	207	16.63
0.9 to 0.95	96	21	117×2	14.38×2

It was essentially impossible to get a reliable estimate of the error in the scanning efficiency, since so few events were double-scanned and since the efficiencies for the elastic events showed a $\cos\theta_{\text{c.m.}}$ dependence. Therefore, the error in each correction was estimated as the square

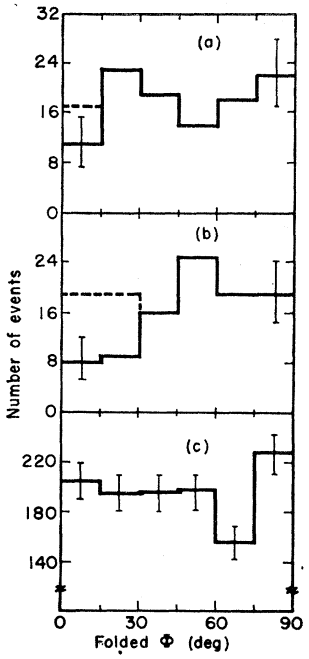

FIG. 7. Histograms of the folded-Φ distribution for the elastic events with (a) $0.85 \leqslant \cos\theta_{c.m.} < 0.90$ (107 events observed), (b) $0.90 \leqslant \cos\theta_{c.m.} \leqslant 0.95$ (96 events observed), and (c) $\cos\theta_{c.m.} \leqslant 0.95$ (1179 events observed). The solid lines are the observed data. The dashed lines show the corrections. Folded-Φ=0 deg lies in the plane perpendicular to the film plane.

root of the correction and was added linearly, as for a bias, to the error in the original data.

Figure 7(c) shows the folded-Φ distribution, before corrections, for all elastic events with $\cos\theta_{c.m.} \leqslant 0.95$.

2. $(p+0)$ *Events*

Distributions both in Φ and folded Φ were made of the outgoing π^+ for various scattering angles of the π^+. All of these were isotropic. More significant tests were the Φ and folded-Φ distributions of the π^+ for all $(p+0)$ events in which the proton stopped in the hydrogen and had a range of less than 2 cm. There were only six such events, and they were randomly distributed both in Φ and in folded Φ. Thus, no biases were found by looking at the 418 $(p+0)$ events as a whole. Furthermore, no bias of any kind was found by studying the events that were double-scanned. Therefore, we calculated scanning efficiencies assuming randomness, and corrected the total number of events for the purpose of estimating branching ratios. This correction was 14 events, making the total number of $(p+0)$ events 432 ± 25. The error, estimated in a manner similar to that used for the elastic events, is $(418)^{1/2}+(14)^{1/2}$.

It is thought that a folded-Φ bias was seen for the elastic events but not for the $(p+0)$ events because elastic scattering includes a diffraction peak which contains a sizeable fraction of events that are hard to see, while single-pion production has no such peak.

3. $(n++)$ *Events*

The two charged outgoing particles were positive pions which did not stop in the chamber. Therefore, all of the $(n++)$ events had outgoing tracks that were long enough to be readily visible on the scanning table, and they did not have to be coplanar, as in the case of elastic events. Thus, the factors that frequently contribute to an azimuthal bias were not present. Furthermore, no bias of any kind was found by studying the events that were double-scanned. Therefore, we calculated scanning efficiencies assuming randomness, which gave a correction of four events to the total number of $(n++)$ events. This gives a corrected total of 79 ± 11 $(n++)$ events. The error is $(75)^{1/2}+(4)^{1/2}$.

E. Normalization

The total path length of the incident pions in this experiment was not measured. Instead, existing total-cross-section measurements were used to normalize the data. There are two recent counter measurements of the π^+-p total cross section over the energy region of this experiment.[1,2] These two experiments show a small systematic difference in the total cross section as a function of energy.

The present experiment has been normalized to the results of Brisson *et al.*,[1] rather than those of Devlin *et al.*[2] This choice was made primarily because it leads to a total elastic cross section that is more consistent with the result of Helland *et al.*[13] However, this decision is still quite arbitrary. Fitting a smooth curve to the data of Brisson *et al.*[1] gives

$$\sigma_{\text{total}}(\pi^+-p)=16.1\pm0.8 \text{ mb}$$

at a beam energy of 600 MeV.

IV. RESULTS AND CONCLUSIONS

A. Elastic Events

After being corrected as explained in Sec. IIID, the angular distribution was fitted to a polynomial in

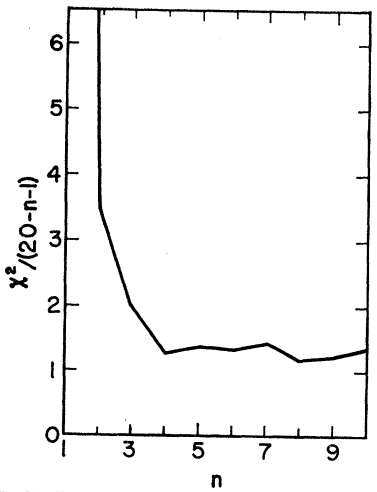

FIG. 8. Chi-square divided by the number of degrees of freedom for the least-squares fit of the polynomial in $\cos\theta_{c.m.}$ to the elastic angular distribution, plotted as a function of the order, n, of the polynomial.

[13] J. A. Helland, T. J. Devlin, D. E. Hagge, M. J. Longo, B. J. Moyer, and C. D. Wood, in *Proceedings of the 1962 Annual International Conference on High-Energy Physics at CERN*, edited by J. Prentki (CERN, Geneva, 1962), p. 3. These authors have tabulated their data in detail in Lawrence Radiation Laboratory Report UCRL-10478, 1962 (unpublished).

$\cos\theta_{\text{c.m.}}$:

$$d\sigma/d\Omega_{\text{c.m.}}=\sum_{k=0}^{n} a_k \cos^k\theta_{\text{c.m.}}.$$

The least-squares fitting was done by an IBM-704 program, PALSI, for all values of n in the interval $1\leqslant n\leqslant 10$.[14] The experimental points are listed in Table I. The errors in the original data were taken as the square root of the number of events, except when there were fewer than 25 events. In the latter case one half of the difference between the upper and lower limits of the 68.3% confidence interval was used, as determined from the Poisson distribution.[15] For numbers above 25 this is very nearly $\sqrt{N}$. As explained in Sec. IIID, when a correction was added to a column, its error and the error in the original data were added linearly.

The χ^2 of the fit divided by the number of degrees of freedom is plotted as a function of n, the order of the polynomial, in Fig. 8. From this figure it is seen that the angular distribution is properly fitted by a fourth-order polynomial. The angular distribution is shown in Fig. 9.

Integrating the area under the fitted curve in Fig. 9 gives 1310±14 elastic events. The error is that due to fitting; it is smaller than $(1310)^{1/2}$ because we have assumed that a fourth-order polynomial in $\cos\theta_{\text{c.m.}}$ fits the shape of the distribution. Using this number of elastics along with the corrected number of $(p+0)$ and $(n++)$ events given in Sec. IIID, we normalized the data to $\sigma_{\text{total}}=16.1\pm0.8$ mb. This gave $\sigma_{\text{elastic}}=11.6\pm0.6$ mb. Table II gives the coefficients of the fitted polynomial in $\cos\theta_{\text{c.m.}}$. The uncertainties given in this table include both the fitting error and the error due to normalization. The two relative errors were combined in quadrature according to the method of propagation of errors.

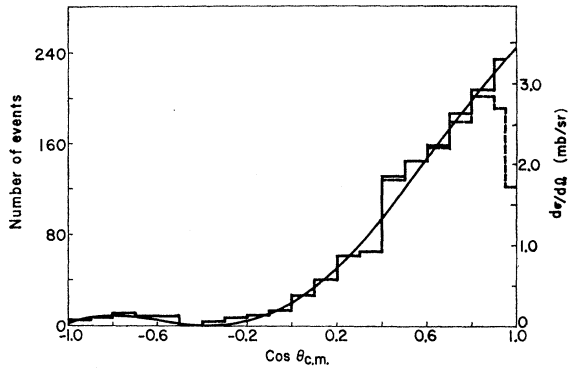

FIG. 9. The angular distribution of the elastic events. The smooth curve is that of the least-squares fitted polynomial of fourth order. It is fitted to the solid-line histogram which runs from −1 to 0.95. (See Table I.) The dashed-line histogram shows the data before correction. The resolution of $\cos\theta_{\text{c.m.}}$ is less than half of the cell width used in the histogram.

TABLE II. The coefficients of the polynomial in $\cos\theta_{\text{c.m.}}$ fitted to the elastic angular distribution. The errors include the uncertainty due to normalization.

a_0 (mb/sr)	a_1 (mb/sr)	a_2 (mb/sr)	a_3 (mb/sr)	a_4 (mb/sr)
0.30±0.03	1.64±0.14	2.53±0.25	0.06±0.22	−1.09±0.31

In Table II the largest coefficients are a_1 and a_2, which is to be expected since the energy of this experiment is still in the region of the $(\frac{3}{2},\frac{3}{2})$ resonance. Since $\cos^4\theta_{\text{c.m.}}$ is required to fit the data, angular-momentum states up to at least D wave must be present. However, the coefficient of $\cos^4\theta$ is negative. If the partial-wave expansion is terminated at the D state and Coulomb scattering is neglected,[16] the coefficient of $\cos^4\theta_{\text{c.m.}}$ can be negative only if both $D_{3/2}$ and $D_{5/2}$ are present (see Appendix). Therefore, at least $J=\frac{5}{2}$ contributes to the angular distribution.

From the curve fitted to the angular distribution of the elastic events (Fig. 9), the differential cross section in the forward direction is

$$d\sigma(0\text{ deg})/d\Omega_{\text{c.m.}}=3.43\pm0.35\text{ mb/sr},$$

where the error includes both the uncertainty due to fitting and that due to normalization. Cronin's evaluation of the real part of the forward-scattering amplitude from dispersion relations[17] together with the optical theorem gives

$$d\sigma(0\text{ deg})/d\Omega_{\text{c.m.}}=2.92\pm0.42\text{ mb/sr}.$$

The main contribution comes from the real part of the forward-scattering amplitude. The error in the real part was taken to be 10%. The dispersion-relation result appears to be consistent with the experimental result.

B. Branching Ratios

From the numbers of events already presented and the total cross section interpolated from the Brisson

TABLE III. Branching ratios and cross sections.

Reaction	Number of events Observed	Number of events After corrections	Branching ratio (%)	Cross section (mb)
$\pi^++p\rightarrow\pi^++p$	1245	1310±14	71.9±0.8	11.6±0.6
$\pi^++p+\pi^0$	418	432±25	23.7±1.4	3.8±0.3
$\pi^++n+\pi^+$	75	79±11	4.3±0.6	0.7±0.1
all others	6[a]		≲1	≲0.2

[a] Six events out of 2494 had more than two outgoing charged prongs.

[14] R. E. von Holdt, PALSI—A Polynomial Approximating Code, Lawrence Radiation Laboratory Report UCRL-5504, 1959 (unpublished).

[15] E. L. Iloff, Interactions and Lifetimes of K Mesons, University of California Radiation Laboratory Report UCRL-3605, 1956 (unpublished) p. 43.

[16] This assumption was checked by making a least-squares fit of the angular distribution in which the three most-forward experimental points (Table I) were omitted. The resulting coefficients agreed well with those shown in Table II. Hence, neglecting Coulomb scattering in the above-mentioned calculation appears to be valid.

[17] J. W. Cronin, Phys. Rev. **118**, 824 (1960).

data, the branching ratios and cross sections were calculated as shown in Table III. The estimated errors are one standard deviation. The errors in the cross sections include the error due to normalization.

C. Inelastic Events

From this experiment we find

$$(p+0)/(n++)=5.5\pm0.8.$$

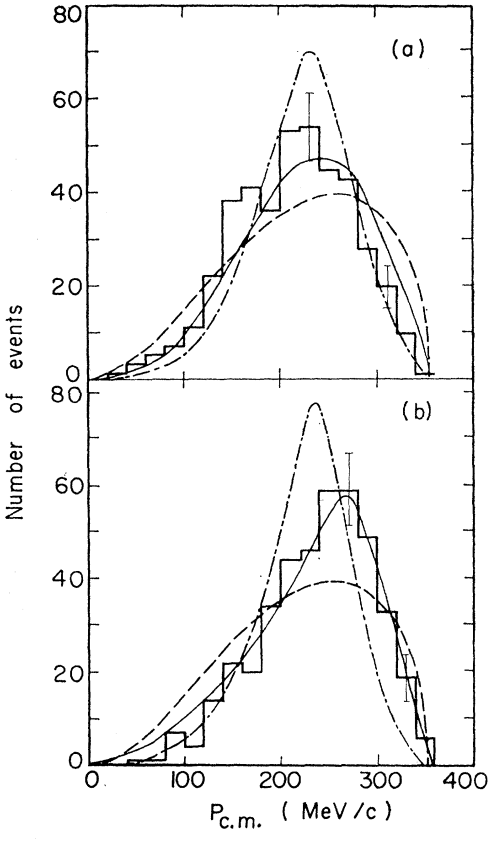

FIG. 10. Momentum spectrum of the (a) π^+ and (b) π^0 for the 418 $(p+0)$ events. Solid lines are for the isobar model of Olsson and Yodh (Ref. 7), the dot-dash lines are for the Sternheimer and Lindenbaum model (Refs. 5, 6), and the dashed curves are phase space. All curves are normalized to equal area.

Of the three isobar models this result agrees best with the value 4.9 predicted by Olsson and Yodh (hereafter call OY),[7] but is also consistent with 6.5 predicted by Sternheimer and Lindenbaum (SL).[6] According to Fig. 2(i) of Ref. 7, however, experimental data at slightly higher energies favor the OY model. Bergia *et al.* (BBS)[5] predict $(p+0)/(n++)=1.8$ at the energy of the present experiment,[7] which does not agree with our result.

1. (p+0) Events

The π^+ and π^0 momentum spectra are shown in Fig. 10(a) and (b), respectively. These histograms are compared to phase space, the SL model (curves are from Ref. 5), and the OY model.[7] The BBS model is not shown because it predicts a large dip in both pion spectra, which definitely disagrees with the experimental data. The OY model fits these spectra best. Their π^0 spectrum fits the data very well; however, their π^+ spectrum is displaced slightly to the right with respect to the histogram.

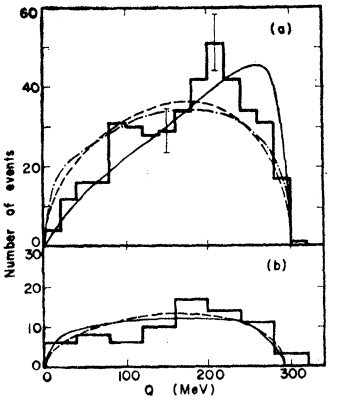

FIG. 11. Distribution of the Q value between two outgoing pions for the (a) 418 $(p+0)$ events and (b) 75 $(n++)$ events. Solid lines are for the Olsson and Yodh model (Ref. 7). Dashed lines are phase space. The dot-dashed line in (a) is for the Sternheimer and Lindenbaum model (Refs. 5, 6). In (b) the Sternheimer and Lindenbaum model and the Olsson and Yodh model are congruent. All curves are normalized to the area of the corresponding histogram.

The $Q(\pi^+,\pi^0)$ distribution is shown in Fig. 11(a). In this histogram there is a definite, although not large, peak centered at 210 MeV. Dalitz plots (not shown) of the 418 $(p+0)$ events show the very broad maxima

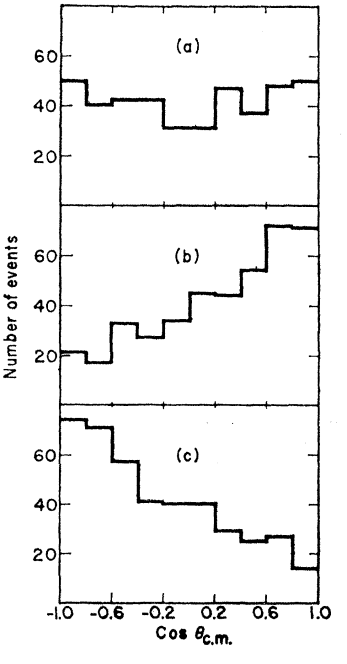

FIG. 12. Distribution of the cosine of the c.m. scattering angle of the (a) π^+, (b) π^0, and (c) proton for the 418 $(p+0)$ events.

of the pion-nucleon isobar, but they do not indicate a $\pi-\pi$ resonance. Therefore, it is very unlikely that the 210-MeV peak in Fig. 11(a) (mass=486 MeV) is a $\pi-\pi$ resonance. The peak is apparently a result of the $(\frac{3}{2},\frac{3}{2})$ pion-nucleon isobar. The $Q(\pi^+,\pi^0)$ distribution fits the OY model very well from 0 to 200 MeV; however, the peak predicted by their model is displaced about 50 MeV with respect to the peak in the histogram. Neither phase space nor the SL model fit the experimental data.

The angular distribution for each of the outgoing particles is shown in Fig. 12. The angular distribution of the π^+ as compared to the other two suggests that the π^+ tends to follow the direction of the proton more frequently than the π^0 does. This is what one would expect from an isobar model, since the π^+ forms the isobar more frequently than the π^0 does.

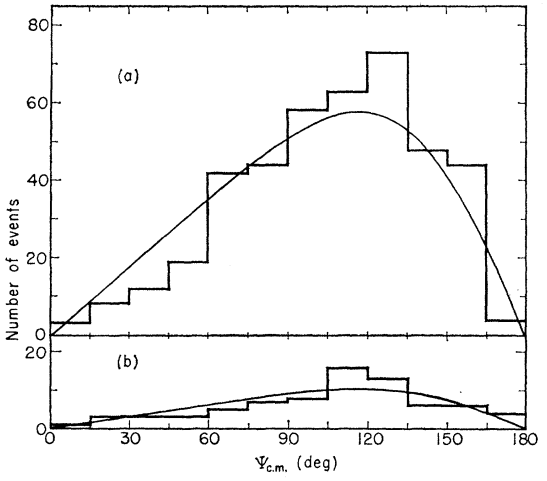

FIG. 13. Distribution of the opening angle between the two outgoing pions in the reaction's c.m. frame for the (a) 418 $(p+0)$ events and (b) 75 $(n++)$ events. Solid curves are phase space.

The distribution of the opening angle between the two pions is shown in Fig. 13(a). It is very similar to phase space.

2. $(n++)$ *Events*

The momentum spectra of the two outgoing pions are shown added together in Fig. 14. In this distribution and in the $Q(\pi^+,\pi^+)$ distribution there is no apparent difference between the SL model and OY model.[18] There are not enough events to tell whether the data favor the isobar models or phase space.

The $Q(\pi^+,\pi^+)$ distribution is shown in Fig. 11(b). Again, there are too few events to give the shape of the spectrum; furthermore, phase space and the isobar models make very similar predictions for the shape of this spectrum.

[18] G. B. Yodh, University of Maryland, College Park, Maryland (private communication).

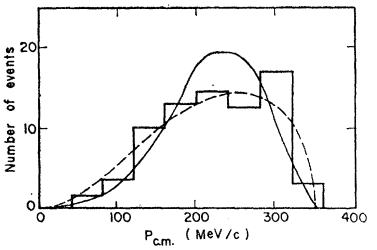

FIG. 14. Combined momentum spectra of the two π^+ mesons for the 75 $(n++)$ events. Thus, there are 150 points in this histogram. The solid curve is for the Olsson and Yodh model (Ref. 7) and also the Sternheimer and Lindenbaum model (Ref. 18). The dashed curve is phase space. All curves are normalized to equal area.

The angular distributions of the outgoing particles are shown in Fig. 15. The distribution of the opening angle between the two outgoing pions is shown in Fig. 13(b). These are very similar to the corresponding distributions for the $(p+0)$ events.

D. Comparison with Other Experiments

As far as we know the present experiment agrees with the previously published data.[13,19,20] The coefficients for the angular distribution (Table II) agree very well with those of Helland *et al.*[13] The $(p+0)$ cross section agrees well with the data of Detoeuf *et al.*[19] This depends directly on the total cross section used to normalize the data; however, even if the present experiment had been normalized to Devlin's results[2] rather than those of Brisson *et al.*,[1] the $(p+0)$ cross section from the present experiment would still have been consistent with the data of Detoeuf *et al.*[19]

A bubble-chamber experiment very similar to the present one has been done by Barloutaud *et al.*[20]; however, they had far fewer events. Their results appear to agree well with the present experiment. The

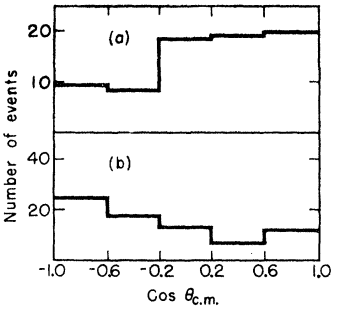

FIG. 15. Histogram of the cosine of the c.m. scattering angle of the (a) two outgoing π^+ mesons and (b) outgoing neutron for the 75 $(n++)$ events. There are 150 points in (a) and 75 points in (b).

[19] J. F. Detoeuf, Y. Ducros, J. P. Merlo, A. Stirling, B. Thevenet, L. van Rossum, and J. Zsembery, in *Proceedings of the 1962 Annual International Conference on High-Energy Physics at CERN* (CERN, Geneva, 1962), p. 5.

[20] R. Barloutaud, L. Cardin, A. Derem, C. Gensollen, A. Leveque, C. Louedec, J. Meyer, and D. Tycho, Nuovo Cimento 26, 1409 (1962).

only discrepancy is that they require only a third-order polynomial in $\cos\theta_{c.m.}$ to fit their elastic angular distribution, whereas the present experiment requires a fourth order; however, this is apparently the result of their comparatively limited statistics (339 elastic events) rather than a disagreement as to the shape of the distribution.

V. SUMMARY

The π^+-p total cross section at 600 MeV is $71.9\pm0.8\%$ elastic and the remainder is almost entirely single-pion production. To fit the elastic angular distribution, partial waves at least up to $D_{5/2}$ are required.

The ratio $(p+0)/(n++)$, the pion momentum spectra for the $(p+0)$ events, and the $Q(\pi^+,\pi^0)$ distribution all appear to be quite well explained by the OY model. The poorest agreement is near the high end of the $Q(\pi^+,\pi^0)$ distribution; nevertheless the Olsson and Yodh model definitely fits the $Q(\pi^+,\pi^0)$ distribution much better than does either phase space or the Sternheimer and Lindenbaum model. There are not enough events in the $(n++)$ distributions to describe the shape of these spectra with sufficient accuracy, but the observed distributions do not contradict either the OY model or the SL model, or for that matter, phase space.

Thus, our single-pion-production events are sufficiently well described by the OY model to conclude that their principal mode of production is through the formation of the $N_{3,3}^*$ resonance. Since the OY model is a refinement of the SL model to which very logical conditions have been added, one would expect the OY model to fit the data better, which it does. Although the BBS model is the framework upon which the OY model was built, the actual BBS spectra do not fit the data.

It would be very interesting to see how well the OY model describes the angular distributions. Adding a second state to the production of the isobar might improve the fit of the π^+ momentum spectrum [Fig. 10(a)] and especially the peak of the $Q(\pi^+,\pi^0)$ distribution. However, this could make the calculations prohibitive.

ACKNOWLEDGMENTS

I would like to thank Professor Wilson M. Powell for the patient guidance he has afforded me during my years as a graduate student, and also Dr. Robert W. Birge for his guidance and encouragement. This experiment was proposed by Dr. John I. Schonle, who contributed extensively during the early stages of the experiment.

I am grateful to Dr. Edward Lofgren and his staff for the use of the Bevatron, and to Professor Luis Alvarez and his group for the use of the bubble chamber. Layton Lynch did a great deal of the scanning. Howard White and his staff provided the data reduction.

The countless hours of work at the scan table described in the section on Acceptance and Classification was done by Miss Charlotte Scales. Miss Scales also did a great deal of work in bookkeeping, plotting graphs, etc.

Conversations regarding the inelastic data with Dr. Zaven Guiragossian and Dr. Julius Solomon are gratefully acknowledged. I thank Professor G. B. Yodh and Dr. M. Olsson for several communications regarding their model.

Mrs. Nancy Wakeman, Mrs. Marleigh Sheaff, and George Bole helped prepare the manuscript.

APPENDIX

For the scattering of spin-zero and spin-$\frac{1}{2}$ particles, there is a nonspin-flip amplitude $f(\theta)$ and a spin-flip amplitude $g(\theta)$. The partial-wave expansions are[3]:

$$f(\theta)=(1/k)\sum_{l=0}^{\infty}[(l+1)A_l^{+}+lA_l^{-}]P_l(\cos\theta)$$

and

$$g(\theta)=(i/k)\sum_{l=1}^{\infty}(A_l^{+}-A_l^{-})P_l^{1}(\cos\theta),$$

where

$$A_l^{\pm}=\frac{\exp[2i\delta_l^{J=l\pm1/2}]-1}{2i}.$$

The δ_l^J are the complex phase shifts. The differential cross section is given by

$$d\sigma/d\Omega=|f|^2+|g|^2,$$

when the spin-$\frac{1}{2}$ particles are unpolarized.

Coulomb effects have been neglected.[16] Also, since the π^+-p system is in a pure $T=\frac{3}{2}$ state, the isotopic-spin label has been suppressed.

Terminating the series at $l=2$ and then substituting into the equation for the differential cross section gives for the coefficient of $\cos^4\theta$

$$(45/4k^2)(|A_2^{+}|^2+4\ \mathrm{Re}A_2^{-}A_2^{+*}).$$

This expression can be negative only if both A_2^{+} and A_2^{-} are nonzero and the phase difference between them is greater than $\pi/2$. Therefore, states up to at least the $D_{5/2}$ state must contribute to the elastic angular distribution.